

# High-Yield Bang Time Detector for the OMEGA Laser

## Introduction

The time interval from the beginning of the laser pulse to the peak of neutron emission (bang time) is an important parameter in inertial confinement fusion (ICF)<sup>1</sup> experiments. The neutron bang time is very sensitive to energy absorption and the subsequent hydrodynamic response of the target and can be directly compared with numerical simulation. Several detectors<sup>2–4</sup> that have been developed to measure the neutron bang time in ICF experiments include a fast (<25-ps) streak-camera-based neutron temporal diagnostic (NTD).<sup>5</sup> An NTD is currently installed on the OMEGA laser<sup>6</sup> at LLE. The NTD streak camera, located at about 3 m from the target, is saturated by neutron yields above  $3 \times 10^{13}$ . OMEGA has produced yields of  $10^{14}$  (Ref. 7), and fast-ignition experiments currently planned<sup>8</sup> at the OMEGA Laser Facility are expected to produce neutron yields above  $10^{14}$ . A new high-yield neutron bang time (HYNBT) detector has been developed at LLE to measure the bang time in these very high yield experiments. The HYNBT has also been developed as a prototype neutron bang time detector for high neutron yields at the National Ignition Facility (NIF). The present work is a continuation of the NIF prototype development published earlier.<sup>9</sup>

## HYNBT Design and Setup

The HYNBT detector design, shown in Fig. 107.19, consists of three chemical-vapor-deposition (CVD) diamond detectors of different sizes and sensitivities placed in a lead-shielded housing. The HYNBT uses commercially purchased<sup>10</sup> “optical-quality” polycrystalline DIAFILM CVD wafers. The HYNBT wafers are disks with the following dimensions: 10-mm diameter, 0.5 mm thick (Ch1); 5-mm diameter, 0.25 mm thick (Ch2); and 2-mm diameter, 0.5 mm thick (Ch3). On each side of the CVD wafer 10 nm of Cr and 50 nm of Au were deposited to provide electrical contact. Each CVD wafer was assembled in an individual aluminum housing with an SMA connector. Figure 107.20 shows the Ch3 housing before and after assembly. Each detector was pre-tested, and the three channels were assembled in a stainless steel cylinder. Figure 107.21 shows the HYNBT before and after assembly. The thin-walled

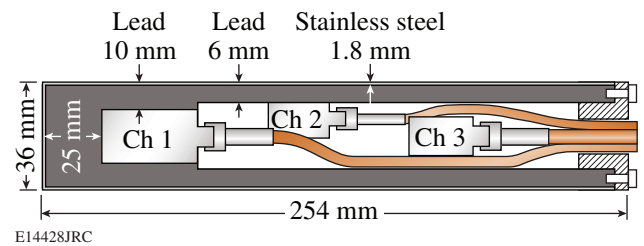


Figure 107.19  
Design of the HYNBT detector.

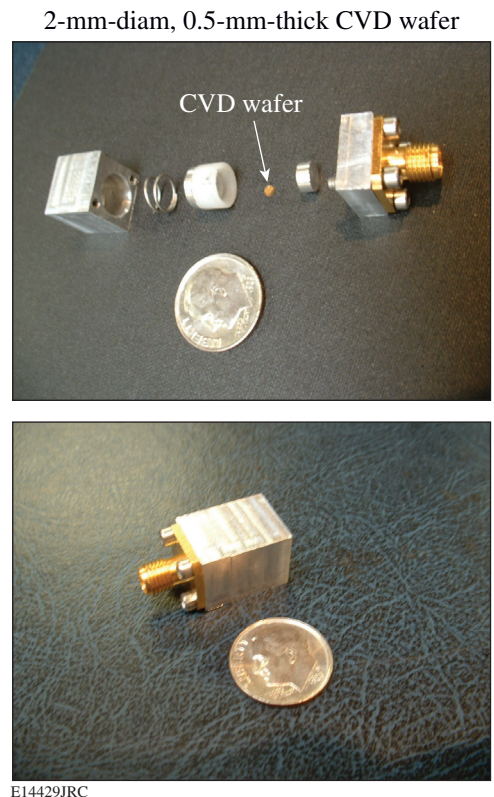


Figure 107.20  
The HYNBT Ch3 housing before and after assembly.

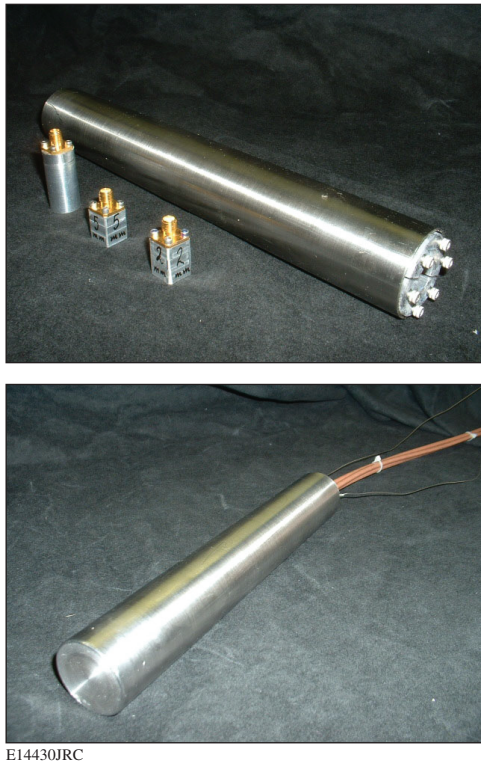


Figure 107.21  
The HYNBT before and after final assembly.

stainless steel cylinder acts as a Faraday cage decreasing the electromagnetic pulse (EMP) noise. Lead shielding inside the steel cylinder protects the CVD diamond detectors from hard x rays. This shielding is not necessary for current experiments on OMEGA and was installed in anticipation of hard x rays produced by the interaction of the short laser pulse with the gold cone or shell in fast-ignition experiments.<sup>8</sup> RG-142 coaxial cables are used because of their double-braid shielding design and low sensitivity to neutrons.<sup>11</sup> The 3-m-long, RG-142 cables are connected to 22-m-long, LMR-400 cables. Inside the OMEGA Target Bay, the cables are routed radially with respect to the target chamber center to minimize the interaction of neutrons with the cables. The bandwidth of the LMR-400 cables is higher than that of the RG-142 cables, but they are much more sensitive to neutrons.<sup>11</sup> This two-cable solution is a compromise between bandwidth and neutron-induced background signals. The HYNBT is deployed in the same re-entrant tube as LLE's NBT,<sup>4</sup> 50 cm from the target chamber center. All of the HYNBT channels were biased at 750 V using a bias-tee (Picosecond Pulse Labs, model 5531). The signals from the HYNBT CVD diamond detectors were recorded on three channels of a 3-GHz, 10-GS/s, Tektronix TDS-694 oscilloscope. The OMEGA optical fiducial pulse

train is recorded on the fourth channel, using a fast photodiode to provide a time reference to the laser. The fiducial analysis and fitting procedure are described in Ref. 4.

### HYNBT Performance

The HYNBT was tested on OMEGA with both DT and D<sub>2</sub> implosions. Figure 107.22 shows typical oscilloscope traces of the three HYNBT channels for a shot yielding  $4.4 \times 10^{12}$  DT neutrons. The measured signals were fit by a convolution of a Gaussian and an exponential decay, as described in Ref. 4. The parameter of the exponential decay represents the collection time of the carriers in the CVD diamond wafer. At a constant bias voltage, the decay parameter depends on the thickness and diameter of the CVD wafer. The optimum decay parameter for

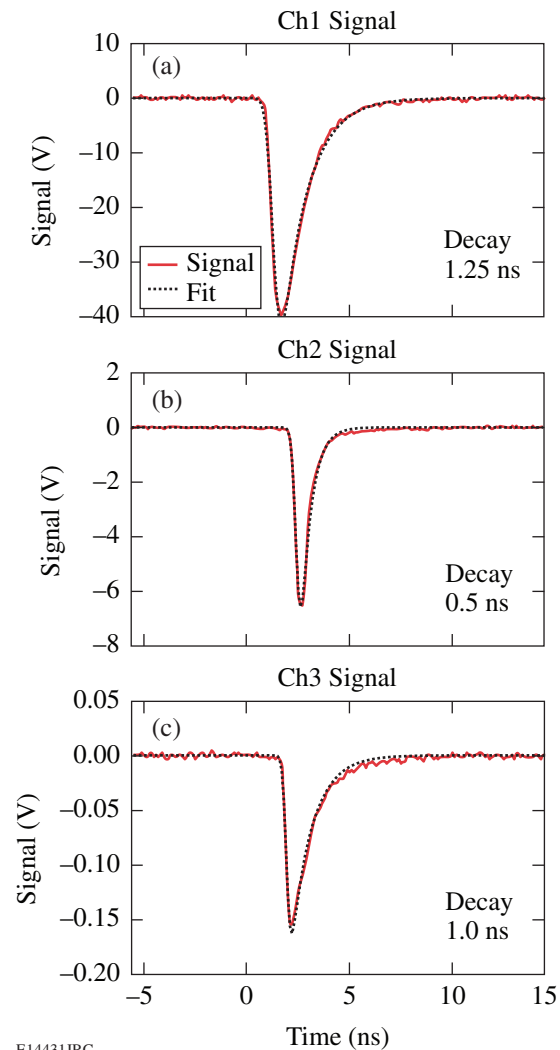


Figure 107.22  
The HYNBT signal for shot 42120 with a DT neutron yield of  $4.4 \times 10^{12}$ .

each HYNBT channel was determined from the fit of a large number of the shots for each channel (low noise, not saturated) and was fixed for the timing analysis of all shots. The Gaussian fit parameters are free parameters for every shot to account for different yields, bang times, ion temperatures, and trigger shifts. The neutron pulse's arrival time is defined to be the center of the Gaussian portion of the fit. Figure 107.23 shows the signal amplitude of three HYNBT channels as a function of DT neutron yield. The straight lines are linear fits to the data for each channel. The first HYNBT channel saturates above a 100-V signal, and the second channel saturates above 80 V. At a yield of  $1 \times 10^{15}$ , the third channel will have a signal of  $\sim 20$  V and will not be saturated. The three HYNBT channels can measure the neutron bang time in DT implosions over the yield range from  $1 \times 10^{10}$  to  $1 \times 10^{15}$ .

The timing accuracy of the HYNBT was studied by measuring the time differences among channels. Figure 107.24(a) shows the time difference between two HYNBT channels recorded on multiple shots over two shot days in May 2005. The DT yields varied from  $8.4 \times 10^{12}$  to  $3.5 \times 10^{13}$ . The rms of the time difference between these two channels is 13 ps. The HYNBT was tested five times during 2005. Figure 107.24(b) shows the time difference between the HYNBT channels appropriate for the neutron yield range during the tests. In November 2005, Ch2 of the HYNBT was used to test a gamma bang time (GBT) detector based on an optical light pipe concept;<sup>12</sup> the time difference between the HYNBT and the GBT had an rms of 15 ps. In all cases the internal time resolution of the HYNBT was better than 20 ps.

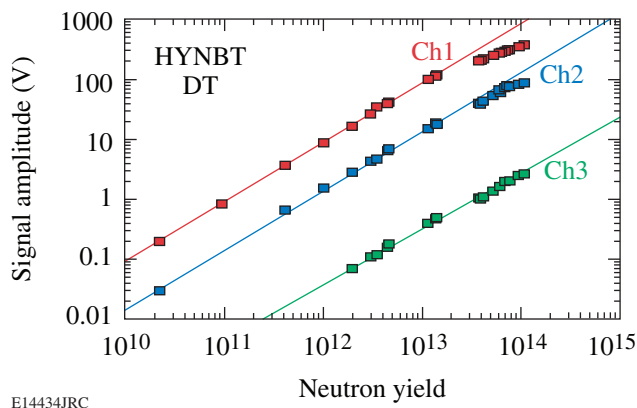


Figure 107.23  
Signal amplitudes of the HYNBT channels.

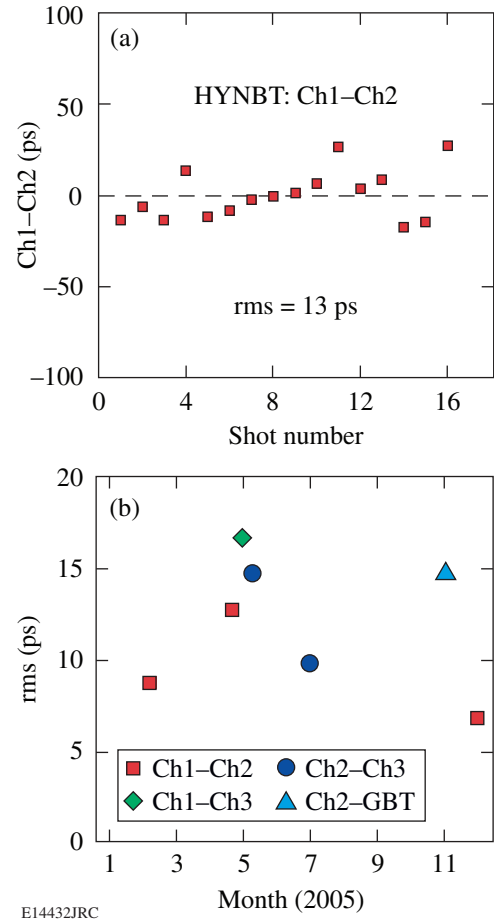


Figure 107.24  
(a) Time difference between HYNBT Ch1 and Ch2 in May 2005; (b) rms of time differences between the HYNBT channels in 2005.

The timing calibration of the HYNBT bang time relative to the OMEGA laser pulse was established by cross-calibration against the NTD.<sup>5</sup> Figure 107.25 shows the cross-calibration of the HYNBT channels and the NTD performed in December 2005, with DT yields varying from  $3.0 \times 10^{12}$  to  $1.4 \times 10^{13}$ . A good correlation between the NTD and the HYNBT is observed with an rms difference of 40 ps. This is larger than the 28-ps rms expected for the difference between two independent measurements, each with a time precision of 20 ps. The discrepancy is explained by direct neutron hits on the NTD, charged-coupled-device (CCD) camera that reduces its temporal resolution.

Although the HYNBT was designed to measure DT neutron bang time, it can also measure bang time in high-yield  $D_2$  shots on OMEGA. Since CVD diamond detectors are less sensitive to  $D_2$  than to DT neutrons, only the first HYNBT channel

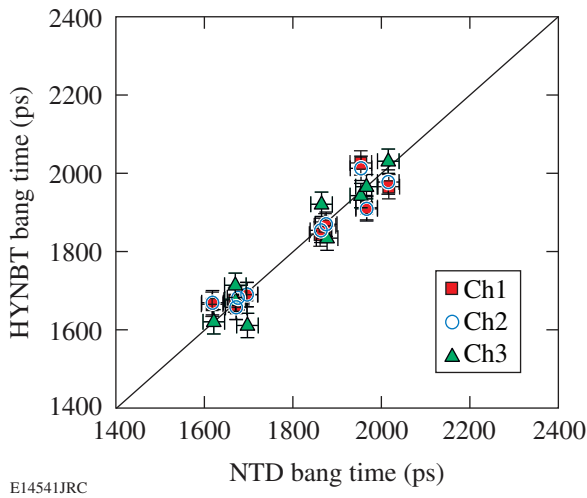


Figure 107.25  
Timing cross-calibration between the HYNBT and the NTD for DT implosions. A line of equal bang times for both instruments is shown for comparison.

is sufficiently sensitive for  $D_2$  implosions on OMEGA. Figure 107.26 shows oscilloscope traces of the first HYNBT channel for shots yielding  $1.1 \times 10^{10}$  and  $9.3 \times 10^{10}$ . At a  $D_2$  yield of  $1 \times 10^{10}$  the signal amplitude is only 10 mV and is affected by EMP and digital noise since the minimum scale setting of the TDS-694 oscilloscope is 10 mV/div. Figure 107.27 shows the first-channel signal amplitude as a function of  $D_2$  yield, and Fig. 107.28 shows the cross-calibration against the NTD. To minimize the influence of noise on the cross-calibration timing, only shots with yields above  $3 \times 10^{10}$  were included. With  $\sim 50$ -ps rms, the  $D_2$  cross-calibration is not as accurate as the DT cross-calibration because most of the signal amplitudes in Fig. 107.28 were below 100 mV.

EMP mitigation techniques used with the HYNBT design reduced the EMP noise to a level about  $10\times$  smaller than that measured with LLE’s NBT.<sup>4</sup> Figure 107.29 shows the EMP noise levels in the least-sensitive Ch3 for different shot conditions. Figure 107.29(a) shows less-than-2-mV noise levels for the standard direct-drive shot. Figure 107.29(b) shows the EMP noise level for a direct-drive shot with backlighting. Backlighting produced additional EMP noise, and for these shot types, the noise level is below 4 mV. The indirect-drive shot with a scale-5/8 hohlraum is shown in Fig. 107.29(c) with the EMP noise below 4 mV. For all shots on OMEGA the EMP noise level in the HYNBT is below 4 mV.

Due to the lead shielding, the HYNBT is insensitive to hard-x-ray signals in direct-drive and most typical indirect-

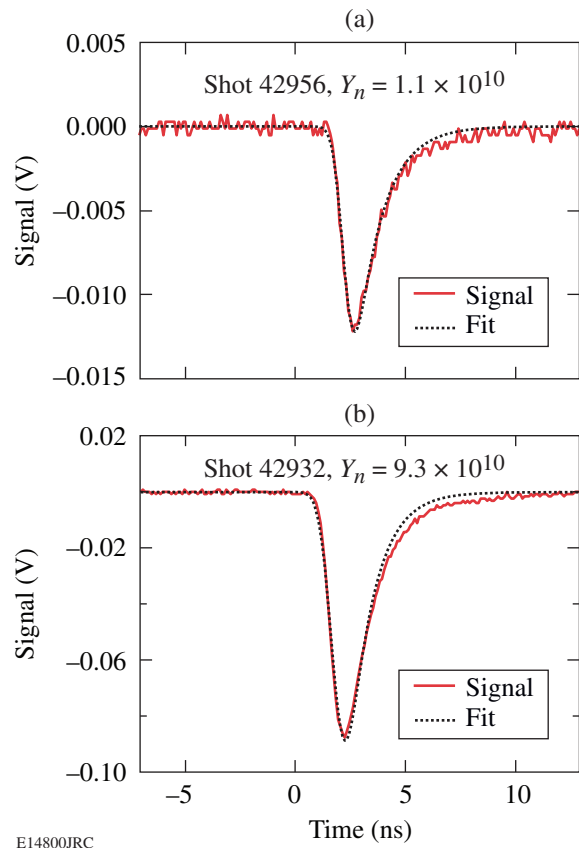


Figure 107.26  
The oscilloscope traces of the first HYNBT channel for  $D_2$  shots: (a) shot 42956 with a yield of  $1.1 \times 10^{10}$ ; (b) shot 42932 with a yield of  $9.3 \times 10^{10}$ .

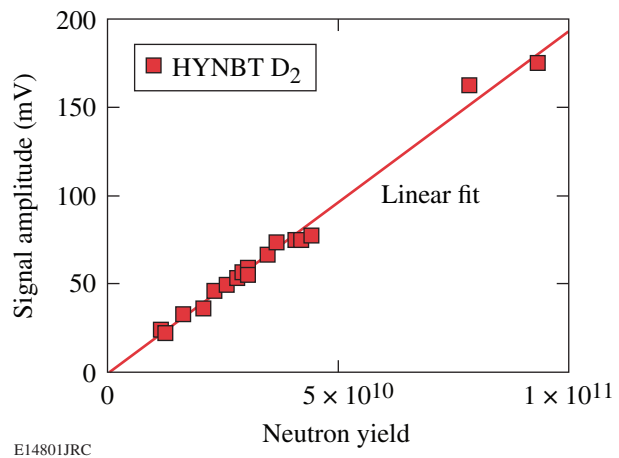
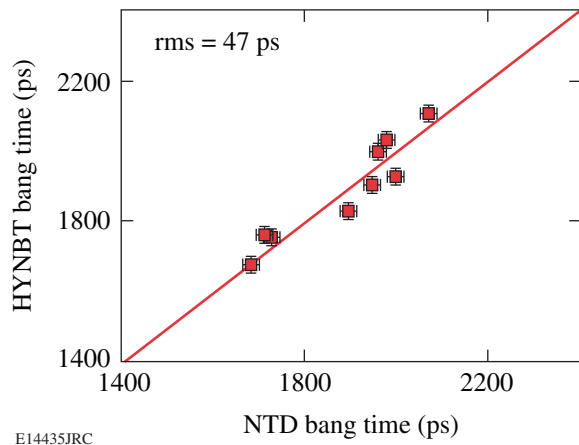


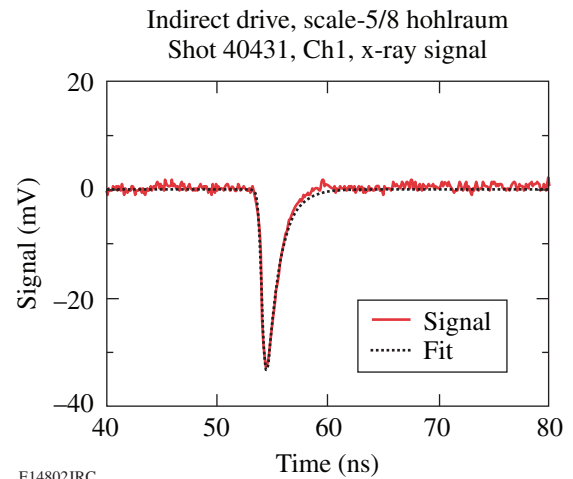
Figure 107.27  
The HYNBT first-channel signal amplitude as a function of  $D_2$  yield.



E14435JRC

Figure 107.28

Timing cross-calibration between the HYNBT first channel and the NTD for  $D_2$  implosions. A line of equal bang time for both instruments is shown for comparison.



E14802JRC

Figure 107.30

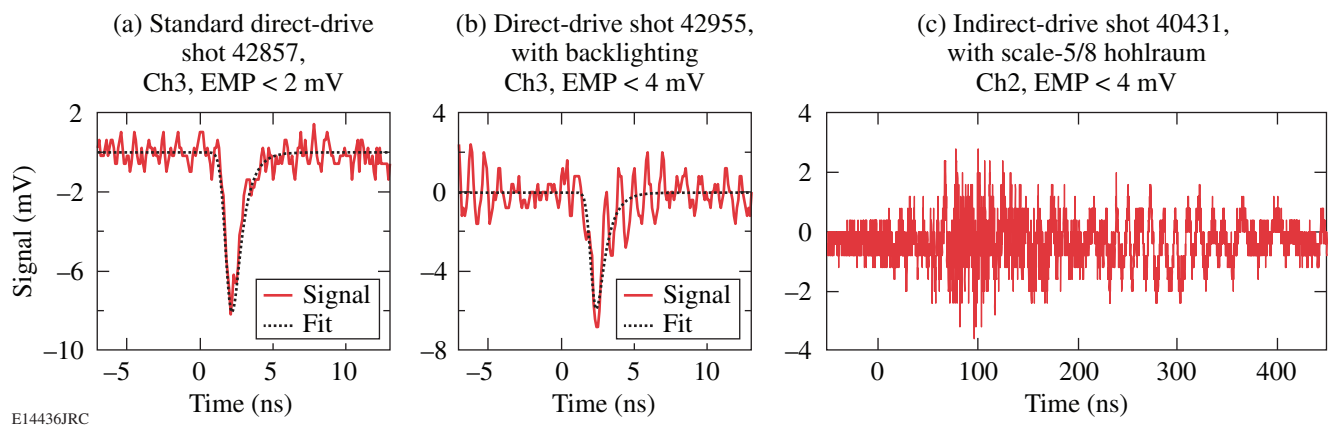
X-ray signal from the scale-5/8-hohlraum, indirect-drive shot 40433 on the HYNBT first channel.

drive shots. Only the most sensitive HYNBT channel was able to record a 30-mV x-ray signal from a scale-5/8 hohlraum, indirect-drive shot that produces  $\sim 100\times$  more hard x rays than direct-drive shots (shown in Fig. 107.30). This relatively low signal is temporally separated from the neutron signal and will not compromise the HYNBT bang time.

### HYNBT on the NIF

The HYNBT was also developed as a prototype neutron bang time detector for the NIF. This is a continuation of earlier work<sup>9</sup> on a NIF bang time prototype. Since publication of this earlier work, the design requirements have changed: Instead of

a low-to-moderate-yield, general-purpose diagnostic, the NIF NBT detector is now required for moderate-to-high yields in the pre-ignition and early-ignition campaigns. At these yields, the original scintillator and photomultiplier channel described in Ref. 9 cannot be used. The NIF NBT is virtually identical to the OMEGA HYNBT with three or four CVD diamond channels. This design will make the NIF NBT more compact, simpler, and less expensive than an NBT employing a photomultiplier. It will be located about 40 to 60 cm from the target in a diagnostic insertion manipulator, together with other NIF diagnostics. In contrast to the OMEGA HYNBT, the shielding on the front of the NIF NBT (facing the target) will be remov-



E14436JRC

Figure 107.29

EMP noise in HYNBT Ch3 for different shots conditions: (a) standard direct-drive shot 42857; (b) direct-drive shot 42955 with backlighting; and (c) indirect-drive shot 40431 with a scale-5/8 hohlraum.

able so that x rays can be used for temporal calibration.<sup>9</sup> The calibration will use x-ray emission from a gold target irradiated by a short laser pulse. The distance from the target, x-ray shielding, and cable length of the HYNBT on OMEGA are comparable to those required on the NIF. The sensitivity of the NIF NBT channels will be comparable to the corresponding HYNBT channels. The dynamic range of the NIF NBT can be increased by increasing the sensitivity of the first channel, decreasing the sensitivity of the third channel, and adding an even less sensitive fourth channel. The first-channel CVD wafer can be changed from a 10-mm-diam, 0.5-mm-thick CVD wafer to a 10-mm-diam, 1-mm-thick CVD wafer. This will increase the sensitivity by a factor of 2, which corresponds to yields of  $2.5 \times 10^{10}$  in  $D_2$  and  $5 \times 10^9$  in DT implosions. If NIF NBT operation will be required at lower yields, the detector can be moved closer to the target. The fourth, least-sensitive channel can be made from a smaller and thinner CVD wafer, from a neutron-hardened CVD wafer, or from a CVD wafer with impurities. All of these factors decrease the sensitivity of the CVD diamonds and shorten the temporal response. The maximum operational yield of the NIF NBT will not be determined by CVD diamond saturation but by neutron-induced signals in the coaxial cables.<sup>11</sup> The study of neutron-induced signals in the coaxial cables will continue on OMEGA. With an optimal cable, the upper-yield range of the NIF NBT is expected to be about  $10^{17}$ .

### Summary

A simple, low-cost, high-yield neutron bang time (HYNBT) detector has been developed and implemented on OMEGA. The HYNBT consists of three chemical-vapor-deposition (CVD) diamond detectors of different sizes and sensitivities placed in a lead-shielded housing. The HYNBT is located in a re-entrant tube 50 cm from the center of the target chamber. The HYNBT has been temporally cross-calibrated against the streak-camera-based neutron temporal diagnostic (NTD) for both  $D_2$  and DT implosions. The HYNBT has an internal time resolution better than 20 ps. The three HYNBT channels can measure the neutron bang time in DT implosions over a yield range of  $1 \times 10^{10}$  to  $1 \times 10^{15}$  and above  $5 \times 10^{10}$  for  $D_2$  implosions. The HYNBT can be implemented on the National Ignition Facility.

### ACKNOWLEDGMENT

This work was supported by the U.S. Department of Energy Office of Inertial Confinement Fusion under Cooperative Agreement No. DE-FC52-92SF19460, the University of Rochester, and the New York State Energy Research and Development Authority. The support of DOE does not constitute an endorsement by DOE of the views expressed in this article.

### REFERENCES

1. J. D. Lindl, *Inertial Confinement Fusion: The Quest for Ignition and Energy Gain Using Indirect Drive* (Springer-Verlag, New York, 1998).
2. R. A. Lerche *et al.*, *Rev. Sci. Instrum.* **59**, 1697 (1988).
3. N. Miyanaga *et al.*, *Rev. Sci. Instrum.* **61**, 3592 (1990).
4. C. Stoeckl, V. Yu. Glebov, J. D. Zuegel, D. D. Meyerhofer, and R. A. Lerche, *Rev. Sci. Instrum.* **73**, 3796 (2002).
5. R. A. Lerche, D. W. Phillion, and G. L. Tietbohl, *Rev. Sci. Instrum.* **66**, 933 (1995).
6. T. R. Boehly, D. L. Brown, R. S. Craxton, R. L. Keck, J. P. Knauer, J. H. Kelly, T. J. Kessler, S. A. Kumpan, S. J. Loucks, S. A. Letzring, F. J. Marshall, R. L. McCrory, S. F. B. Morse, W. Seka, J. M. Soures, and C. P. Verdon, *Opt. Commun.* **133**, 495 (1997).
7. J. M. Soures, R. L. McCrory, C. P. Verdon, A. Babushkin, R. E. Bahr, T. R. Boehly, R. Boni, D. K. Bradley, D. L. Brown, R. S. Craxton, J. A. Delettrez, W. R. Donaldson, R. Epstein, P. A. Jaanimagi, S. D. Jacobs, K. Kearney, R. L. Keck, J. H. Kelly, T. J. Kessler, R. L. Kremens, J. P. Knauer, S. A. Kumpan, S. A. Letzring, D. J. Lonobile, S. J. Loucks, L. D. Lund, F. J. Marshall, P. W. McKenty, D. D. Meyerhofer, S. F. B. Morse, A. Okishev, S. Papernov, G. Pien, W. Seka, R. Short, M. J. Shoup III, M. Skeldon, S. Skupsky, A. W. Schmid, D. J. Smith, S. Swales, M. Wittman, and B. Yaakobi, *Phys. Plasmas* **3**, 2108 (1996).
8. C. Stoeckl, J. A. Delettrez, J. H. Kelly, T. J. Kessler, B. E. Kruschwitz, S. J. Loucks, R. L. McCrory, D. D. Meyerhofer, D. N. Maywar, S. F. B. Morse, J. Myatt, A. L. Rigatti, L. J. Waxer, J. D. Zuegel, and R. B. Stephens, *Fusion Sci. Technol.* **49**, 367 (2006).
9. V. Yu. Glebov, C. Stoeckl, T. C. Sangster, S. Roberts, R. A. Lerche, and G. J. Schmid, *IEEE Trans. Plasma Sci.* **33**, 70 (2005).
10. Harris International, New York, NY 10036.
11. V. Yu. Glebov, R. A. Lerche, C. Stoeckl, G. J. Schmid, T. C. Sangster, J. A. Koch, T. W. Phillips, C. Mileham, and S. Roberts, presented at ICOPS 2005, International Conference on Plasma Sciences, Monterey, CA, 20–23 June 2005 (Paper 10281).
12. M. Moran, G. Mant, V. Glebov, C. Sangster, and J. Mack, presented at the 16th Annual Conference on High-Temperature Plasma Diagnostics, Williamsburg, VA, 7–11 May 2006 (Paper TP22).